Using X-ray Absorption Spectroscopy to Measure Changes of Electronic Structure Accompanying Lithium Insertion into the Perovskite Type Oxides

Masanobu Nakayama, Kazuomi Imaki, Wonkyung Ra, Hiromasa Ikuta, Yoshiharu Uchimoto, and Masataka Wakihara*

Department of Applied Chemistry, Tokyo Institute of Technology, Ookayama, Meguro-ku, Tokyo 152-8552, Japan

Received July 18, 2002. Revised Manuscript Received February 20, 2003

The changes of electronic structure accompanying the electrochemical and thermal insertion of lithium into the perovskite type oxide, $La_{1/3}NbO_3$, have been investigated by using X-ray absorption spectroscopy (XAS) techniques. In the electrochemical lithium insertion process, spectra of Nb L_{III}-edge and La L_{III}-edge revealed that the reduction can be ascribed to the variation of oxidation states from Nb^{5+} to Nb^{4+}, and La^{3+} does not contribute to the reduction reaction. Furthermore, the O K-edge spectrum does show change with electrochemical lithium insertion. From the results of Nb L_{III}-edge and O K-edge spectra with thermal lithium insertion and first principles molecular orbital calculations, oxygen 2p orbital partially contributes the charge compensation, and the oxide ions near the inserted lithium ions are ionized strongly.

Introduction

Transition-metal oxides having lithium insertion sites are particularly interesting for use as the cathode material of lithium ion batteries with high-energy density.[1] These materials are attractive not only for commercial use, but also for use as a model material for the basic study of solid-state electrochemical reaction, because the host crystal structure is almost the same before and after an electrochemical reaction. Therefore, such model materials are suitable for theoretical treatment, such as first principles molecular orbital calculation,[2−6] lattice gas model simulation,[7] and so on.[8,9] A-site-deficient perovskite type oxide, $La_{1/3}NbO_3$, is considered to be a candidate for these model compounds because of the following structural features: (i) $La_{1/3}NbO_3$ has a large amount of vacancies in A-site, and the lithium ions can be inserted into A-site vacancies; and (ii) this compound has a structure with relatively high symmetry. In addition, it is known that there are two types of lithium insertion reactions in this perovskite type compound: electrochemical Li^+ insertion reaction, eq 1[10,11]; and thermal Li^+ insertion reaction, eq 2[12,13]. (The latter is expressed more accurately as the substitution of Li^+ for La^{3+} in perovskite A-site.)

$$x\mathrm{Li} + \mathrm{La}_{1/3}\mathrm{NbO}_3 \rightarrow \mathrm{Li}_x\mathrm{La}_{1/3}\mathrm{NbO}_3 \quad (1)$$

$$^{y}/_{2}\ \mathrm{Li}_2\mathrm{O} + (1-y)\ \mathrm{La}_{1/3}\mathrm{NbO}_3 + {}^{y}/_{2}\ \mathrm{Nb}_2\mathrm{O}_5 \rightarrow \mathrm{Li}_y\mathrm{La}_{(1-y)/3}\mathrm{NbO}_3 \quad (2)$$

The reaction shown in eq 1 is classified as a redox reaction, and it is considered in a conventional chemical sense that the Nb^{5+} ion is reduced to the Nb^{4+} ion. On the other hand, the reaction described in eq 2 does not accompany a redox reaction, therefore the Nb^{5+} ion does not change its oxidation state. Hereinafter in this paper, x means the molar composition of electrochemically inserted lithium ions, and y means the molar amount of substitution $3Li^+$ for La^{3+}, or thermally inserted lithium ions.

The crystal structure of pristine $La_{1/3}NbO_3$ was first described by Iymer and Smith.[14] As shown in Figure 1, La ions and vacancies at A-sites are ordered within alternate (001) planes doubling the c-parameter of the cubic perovskite-type cell and leading to a slightly distorted orthorhombic lattice with parameters $a \sim a_p$, $b \sim b_p$, $c \sim 2a_p$ (p refers to the cubic-perovskite unit cell).

The electrochemical insertion of lithium in $La_{1/3}NbO_3$ has been reported by Nadiri et al.,[10] and they confirmed

* Corresponding author. Phone: + 81 3 5734 2145. Fax: +81 3 5734 2146. E-mail: mwakihar@o.cc.titech.ac.jp.

(1) *Lithium Ion Batteries*. Wakihara, M., Yamamoto, O., Eds.; Kodansha: Tokyo, 1998.
(2) Zheng, T.; Dahn, J. R. *Phys. Rev. B* **1997**, *56*, 3800.
(3) Aydinol, M. K.; Kohan, A. F.; Ceder, G.; Cho, K.; Joannopoulos, J. *Phys. Rev. B* **1997**, *56*, 1354.
(4) Koyama, Y.; Kim, Y.-S.; Tanaka, I.; Adachi, H. *Jpn. J. Appl. Phys.* **1999**, *38*, 2024.
(5) Hibino, M.; Han, W.; Kubo, T. *Solid State Ionics* **2000**, *135*, 61.
(6) Liu, Y.; Fujiwara, T.; Yukawa, H.; Morinaga, M. *Electrochim. Acta* **2001**, *46*, 1151.
(7) Gao, Y.; Reimers, J. N.; Dahn, J. R. *Phys. Rev. B* **1996**, *54*, 3878.
(8) Goodenough, J. B.; Manthiram, A.; Wnetrzewski, B. *J. Power Sources* **1993**, *43*−*44*, 269.
(9) Yamaki, J.; Egashira, M.; Okada, S. *J. Power Sources* **2001**, *97*−*98*, 349.
(10) Nadiri, A.; Le Flem, G.; Delmas, C. *J. Solid State Chem.* **1988**, *73*, 338.
(11) Nakayama, M.; Imaki, K.; Ikuta, H.; Uchimoto, Y.; Wakihara, M. *J. Phys. Chem. B* **2002**, *106* (25), 6437.
(12) Belous, A. G.; Didukh, I. R.; Novosadova, E. B.; Pashkova, E. V.; Khomenko, B. S. *Izv. Akad. Nauk SSSR, Neorg. Mater.* **1990**, *26*, 1294.
(13) Kawakami, Y.; Ikuta, H.; Wakihara, M. *J. Solid State Electrochem.* **1998**, *2*, 206.
(14) Iyer P. N.; Smith, A. J. *Acta Crystallogr.* **1967,** *23*, 740.

10.1021/cm020741u CCC: $25.00
Published on Web 03/26/2003

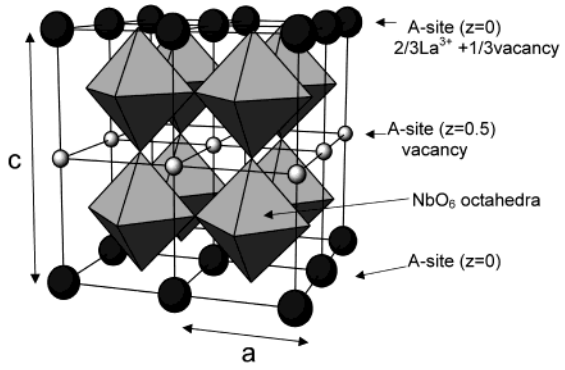

Figure 1. Structure of $La_{1/3}NbO_3$.

by X-ray diffraction that the host structure of $La_{1/3}NbO_3$ is maintained during the insertion reaction. Dilanian et al.[15] investigated the crystal structure of chemically lithiated perovskite oxides, $Li_xLa_{1/3}NbO_3$ using a neutron diffraction technique. We have recently investigated the electrochemical behavior associated with Li insertion into the solid solution $Li_yLa_{(1-y)/3}NbO_3$, and concluded that the cell potential with Li^+ insertion was strongly dependent on the arrangement of La^{3+} and Coulombic interaction.[11] And, these three reports[10,11,15] revealed that the inserted lithium ions reside at vacant A-site.

On the other hand, the variation of oxidation states for each element through the Li^+ insertion reaction is still uncertain. In the classical view, because these electrochemical redox reactions have been thought to keep the octet rule,[16] only the transition metal can react as a redox species. However, some reports have suggested that the redox reaction occurs not only at transition metal ions but also at oxide ions, as determined by using the first principles molecular orbital calculation[3,4] or an XAS technique.[17] In this study, we investigate the variation of oxidation states of each ion through the lithium insertion reaction, expressed as eqs 1 and 2, by using the combination of XAS measurement and first principles molecular orbital calculation.

Experimental Section

Different compositions of the $Li_yLa_{(1-y)/3}NbO_3$ ($y = 0$, 0.1, 0.25) solid solution were prepared by conventional solid-state reaction. As described in ref 13, the mixture of stoichiometric amounts of Li_2CO_3 (3N), La_2O_3 (3N), and Nb_2O_5 (3N), (Soekawa Chemical Industries, Ltd.) was heated at 800 °C for 2 h and then at 1200 °C for 24 h in air with several intermittent grindings. In the case of $La_{1/3}NbO_3$ ($y = 0$) it was synthesized at 1300 °C to obtain single phase samples. Crystalline phase identification and the evaluation of lattice parameters were carried out by powder X-ray diffraction using a Rigaku RINT2500V diffractometer with Cu Kα radiation and a curved graphite monochromator, and the results were consistent with our previously reported data.[13] The molar ratio of the metals in the compounds was determined by inductively coupled plasma (ICP) spectroscopy. The samples were dissolved in HCl (35 wt %) solution. Samples (10 mg) and 5 mL of HCl were sealed into a quartz glass tube and heated at 200 °C for 24 h. Because the obtained composition shows good agreement between analytical and nominal compositions within experimental error, nominal compositions will be used in this paper.

Electrochemical reaction of Li insertion was carried out using a three-electrode cell. Li foil (Aldrich) was used as counter and reference electrodes, and a 1 M solution of $LiClO_4$ in anhydrous ethylene carbonate (EC) and diethylene carbonate (DEC) was used as electrolyte (Tomiyama Pure Chemical Company, Ltd.). The working electrode was a mixture of 90 wt % perovskite powders, 7 wt % acetylene black as a current collector, and 3 wt % poly(tetrafluoroethylene) (PTFE) binder. Li foils and the mixture of working electrode were pressed onto Ni-mesh. Electrochemical lithium insertion was carried out by a galvanostatic method (current density 40 $\mu A/cm^2$) using a Hokuto HD-110mSM6 electrochemical interface. The composition of prepared samples was $Li_xLa_{1/3}NbO_3$ ($x = 0.1$, 0.2, 0.4, 0.6, 0.8). The preparation of the cells and electrochemical experiments were performed in an Ar-filled glovebox. The crystalline phase identification of the samples obtained by the electrochemical technique was carried out by powder X-ray diffraction with Cu Kβ radiation. The samples were covered with polyethylene film in an Ar-filled glovebox to prevent reactions with moisture. The electron corrector Ni is used as the internal standard for the correction of peak shifts.

The XAS measurements for the La L_{III}-edge spectra were carried out by transmission mode using synchorotron radiation at the beam line BL-9A, Photon Factory, High Energy Accelerator Research Organization in Tsukuba, Japan. The absorption of Cu K-edge was used for calibration of the absolute energy scale. The pellets of samples after electrochemical treatment were sealed in polyethylene bags to avoid exposure in the air. The XAS measurements of Nb L_{III}-edge and O K-edge spectra were carried out using synchrotron radiation at the beam lines BL-7A and BL-8B1, respectively, at UVSOR, Institute for Molecular Science in Okazaki, Japan. The absorption was determined by the total-electron-yield method. The total yield was divided by the storage-ring current that was recorded simultaneously. The absolute energy scale was determined by comparison with data of the standard material Nb_2O_5. For the samples after electrochemical treatment, all installation operations were performed under Ar or N_2 atomosphere.

Results and Discussion

Figure 2 shows the cell potential under low galvanostatic current (40 $\mu A/cm^2$) through the electrochemical lithium insertion and extraction. From Figure 2b, the charge−discharge curves show that the Li ions reversibly insert/extract the perovskite sample. The detailed insertion site of lithium ion has already been reported in ref 11. The arrows in Figure 2a indicate the samples for XAS measurements. The cell potential of the sample at the composition $x = 0.8$ is lower than 1.0 V where the lithium insertion into acetylene black occurred.[11] Therefore, the sample at $x = 0.8$ is thought to be filled up with electrochemically inserted lithium ions at the vacant A-site. Figure 3 shows the powder XRD patterns for the samples obtained by electrochemical Li insertion. The peak feature of the patterns was roughly unchanged with Li insertion, indicating the host structure keeps its framework upon Li insertion. In detail, the peaks of (200) and (004) were incorporated during Li insertion reaction (similar behavior also observed in the peaks of (114) and (122)), indicating that half of the *c*-axis became closer to the *a*-axis (Figure 1). According to Nadiri et al,[10] similar behavior has been already reported, and the ratio of evaluated lattice parameter *c*/*a* varies a little from 2.022 ($x = 0$) to 2.016 ($x = 0.8$).

Results of XAS measurements for the samples of electrochemical lithium insertion are shown in Figure

(15) Dilanian, R. A.; Yamamoto, A.; Izumi, F.; Kamiyama, T. *Mol. Cryst. Liq. Cryst.* **2000**, *341*, 225.

(16) Shriver, D. F.; Atkins, P. W.; Langford, C. H. *Inorganic Chemistry*, 2nd ed. Oxford University Press: New York, 1994; Ch. 1 and 2.

(17) Kuiper, P.; Kruizinga, G.; Ghijse, J.; Sawatzky, G. A.; Verweij, H. *Phys. Rev. Lett.* **1989**, *62*, 221.

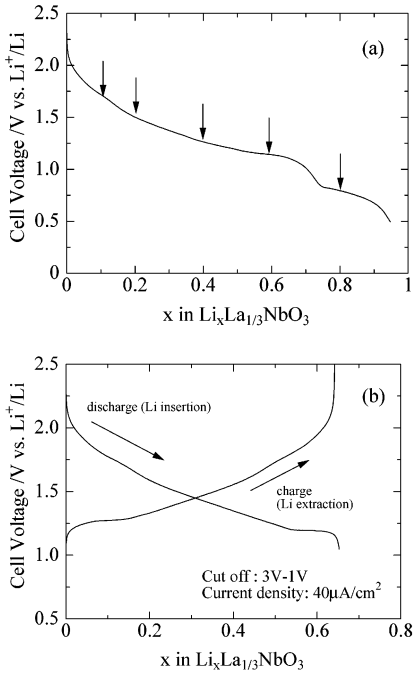

Figure 2. (a) Variation of the cell voltage with electrochemical insertion (current density 40 μA/cm^2). The arrow indicates the samples for the XAS measurement. (b) Variation of the cell voltage with electrochemical Li insertion and extraction.

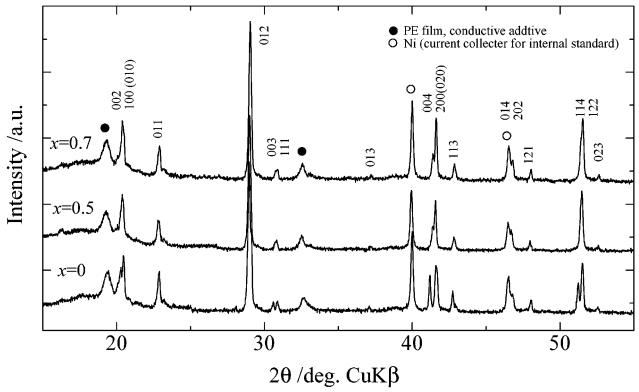

Figure 3. Variation of the powder X-ray diffraction patterns of the perovskite compounds $Li_xLa_{1/3}NbO_3$ with electrochemical lithium insertion. Solid circles indicate the peaks due to the polyethylene film, conductive additives, and PTFE. The peaks with open circles are Ni which was added as the internal standard material. The broad hump around 20° is ascribed to the signal of the polyethylene film.

4. La L_{III}-edge spectra (Figure 4a) of the XAS measurements show no marked change, and formal charges of La ions in perovskite samples are +3 because the spectra of perovskite samples were consistent with that of La_2O_3. This indicates that the oxidation states of La ions at A-site were unchanged through the reaction. The Nb L_{III}-edge spectra (Figure 4b) show two absorption peaks at the composition $x = 0$. Applying the crystal field theory[18] to the NbO_6 octahedra, the energy levels of the Nb 4d orbital were split into two levels, i.e., three degenerate t_{2g} level and two degenerate e_g level, respectively, and the two observed peaks are ascribed to the two levels. As shown in Figure 4b the intensity of the lower energy peak corresponding to the t_{2g} level decreased with increasing the composition of x. Because the XAS spectra reflect the density of state for the unoccupied electron orbital, the decrease of peak intensity corresponds to accepting the electron into the t_{2g} orbital by reduction reaction and decreasing transition probability from $2p^{3/2}$ electrons to t_{2g} orbital. Therefore, such behavior indicates that the reduction from Nb^{5+} to Nb^{4+} occurs along with electrochemical lithium insertion. Figure 4c shows the O K-edge spectra of the samples with composition x. Concerning the selection rule for the absorption spectra, the peaks should be assigned as the O 3p conduction band and/or the metal−oxide molecular orbital hybridized conduction band. In Figure 4c, the spectra can be separated into two regions at 535 eV. In the region above 535 eV, rather broad peaks were observed, and it was generally known that these peaks corresponded to the O 3p conduction band. For example, Nakai et al.[19] have reported the O K-edge XAS spectra of MgO, and the spectra show a broad peak above 535 eV. Because MgO does not have a d-electron band around Fermi energy, it is concluded that the peak above 535 eV reflects the O 3p band. A similar result was also obtained by a multiple-scattering calculation.[20] The peaks at the region less than 535 eV are relatively sharp and change with insertion. According to the spectra of MgO[19] without d-electron, no absorption peaks exist in this region; hence, these peaks are ascribed to the metal−oxide hybridized conduction band. Two peaks were observed at the composition $x = 0$ in the range from 525 eV to 535 eV. However, the two peaks disappeared with electrochemical Li insertion, and an additional peak appeared at about 532 eV. From the variation of O K-edge spectra, the electronic structure of oxide ion changes with Li insertion reaction. The electronic structure of oxide ion would be affected by the interaction of neighboring cations, and there are three kinds of cations interacting with oxide ion: Nb at perovskite B-site, and La and Li at perovskite A-site. It is considered that the interaction between La and O does not affect the changes of electronic structure of oxide ions, because the electronic structure of La ions does not change with Li insertion as mentioned above. Hence, the changes of electronic structure of oxide ions will be explained by two hypotheses. The first hypothesis is that changes of the interaction of Nb−O, or changes in oxidation state of niobium ions from Nb^{5+} to Nb^{4+} (Figure 4b), affect the electron orbital of neighboring oxide ions. From the later discussion on the first principles molecular orbital calculation, the bond between niobium and oxygen has a rather covalent character compared to those of Li−O and La−O. Therefore, such a change of O K-edge spectra corresponds to the fact that the electronic transfer occurred at Nb−O hybridized orbital during the electrochemical Li insertion reaction, or that the oxide ions also partially contribute to the reduction reaction. The second hypothesis is that the change in electron structure of oxide ions is due to the increasing Li−O interaction with increasing the amount of x. Lithium ion is known to

(18) Shriver, D. F.; Atkins, P. W.; Langford, C. H. *Inorganic Chemistry*, 2nd ed. Oxford University Press: New York, 1994; Ch. 6.

(19) Nakai, S.; Mitsuishi, T.; Sugawara, H.; Maezawa, H.; Matsukawa, T.; Mitani, S.; Yamasaki, K.; Fujikawa, T. *Phys. Rev. B* **1987**, *36*, 9241.

(20) Linder, T.; Sauer, H.; Engel, W.; Kambe, K. *Phys. Rev. B* **1986**, *33*, 22.

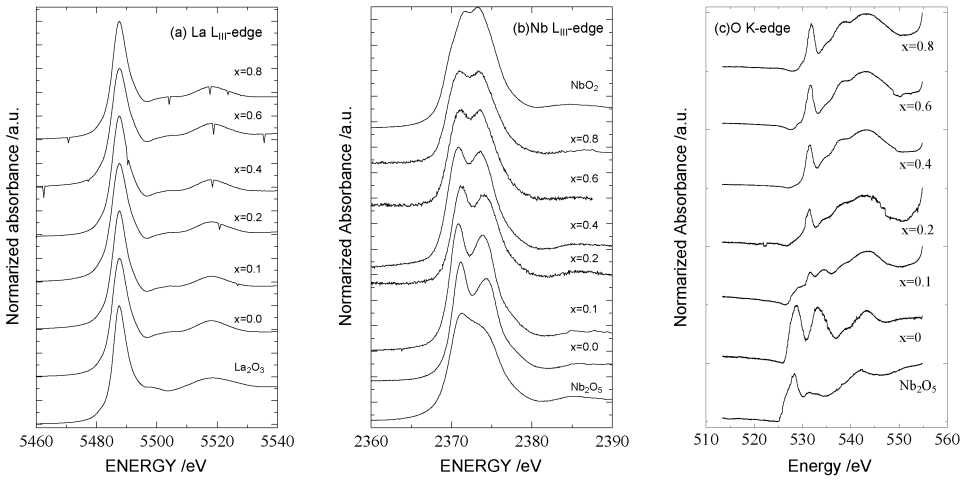

Figure 4. Variation of XAS spectra with electrochemical lithium insertion for the samples $Li_xLa_{1/3}NbO_3$: (a) La L_{III}-edge; (b) Nb L_{III}-edge; and (c) O K-edge.

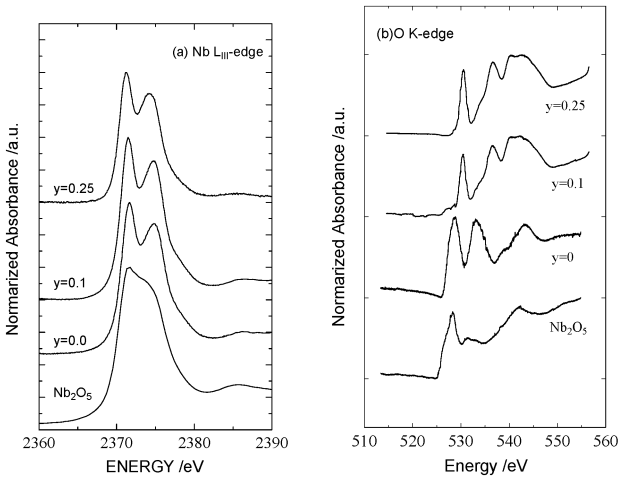

Figure 5. Variation of XAS spectra with thermal lithium insertion for the samples $Li_yLa_{(1-y)/3}NbO_3$: (a) Nb L_{III}-edge; and (b) O K-edge.

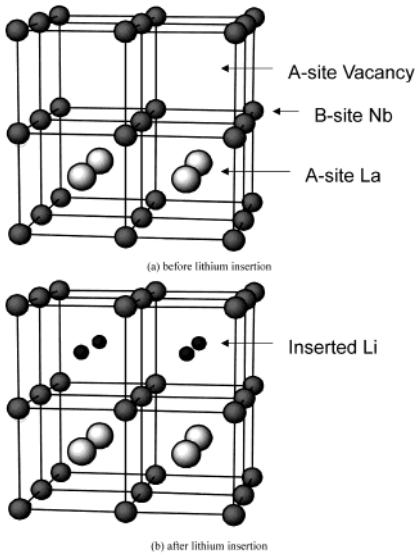

Figure 6. Structure of the samples (a) before and (b) after lithium insertion used for DV-Xα calculation. (Oxide ions are omitted in this figure for simplification).

have a strong ionic character, hence it is considered that the inserted Li ion causes the neighboring oxide ions to become more ionic. Therefore, the changes of ionicity for oxide ion would result in the changes of electronic structure at oxide ion as shown in the O K-edge spectra.

To clarify the reason for the change of O K-edge spectra, we investigated the XAS spectra of samples with thermally inserted Li^+ and also investigated the electron density change using first principles molecular orbital calculation.

Figure 5 shows the Nb L_{III}-edge and O K-edge XAS spectra for the samples with thermally inserted Li^+, $Li_yLa_{(1-y)/3}NbO_3$. In this system, the net redox reaction did not occur (see eq 2), and Nb ions kept their formal oxidation state as +5 through the lithium insertion. Therefore, unaltered XAS spectra of Nb L_{III}-edge (Figure 5a) would be explained as mentioned above. On the other hand, the O K-edge spectra (Figure 5b) vary with thermal Li^+ insertion without reduction of niobium ions and similar to the spectra for the samples with electrochemical Li^+ insertion (Figure 4c). Accordingly the origin of variation of electronic structure of oxide ions is due to the interaction between lithium ion and oxide ion, or the variation of ionicity of oxide ions.

Finally, we will take account of the effect of the structural changes for the XAS spectra during the Li insertion. As shown in Figure 3 and from the refs 10, 12, 13, and 15, the basic framework of perovskite structure was unchanged upon electrochemical or thermal Li insertion. The cell volume change is quite small (~0.2% of cell volume increase for electrochemical reaction (x = 0 to 0.8),[10] and ~1.0% of cell volume decrease for thermal reaction (y = 0 to 0.25)[12] per ABO_3 perovskite unit cell). Furthermore, although the cell volume change showed different tendencies (during Li insertion, the electrochemical one showed expansion of the cell, but the thermal one showed contraction), the O K-edge XAS spectra for both the electrochemical- and thermal-Li-inserted samples varied in similar ways. Therefore, it is concluded that the structural change is not the main reason for the variation of XAS spectra with Li insertion.

The first principles molecular orbital calculation was carried out usinga DV-Xα method.[21,22] The computer

(21) Averill, F. W.; Ellis, D. E. *J. Chem. Phys.* **1973**, *59*, 6412.
(22) Ellis, D. E.; Adachi, H.; Averill, F. W. *Surf. Sci.* **1976**, *58*, 497.

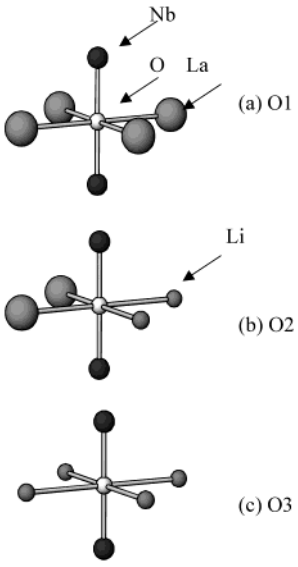

Figure 7. Arrangement of cations linked with three kinds of oxide ions: O1, O2, and O3.

Table 1. Parameters of Modeled Crystal Structure and Ion Distribution for the Calculation of DV-Xα Method

$Li_xLa_{1/3}NbO_3$
space group: *P*4/*mmm* (No. 123)
lattice parameter: $a = b = c/2 = 3.93$, $\alpha = \beta = \gamma = 90°$

site	label/atom	fractional coordinates
1*a* (A_{La})	La/La	(0, 0, 0)
1*b* (A_{vac})	Li/Li	(0, 0, 1/2)
2*h*	Nb/Nb	(1/2, 1/2, 1/4)
4*i*	O1/O	(1/2, 0, 1/4)
1*c*	O2/O	(1/2, 1/2, 0)
1*d*	O3/O	(1/2, 1/2, 1/2)

code SCAT[23] was employed, and Figure 6 and Table 1 show the modeled cluster before and after the lithium-insertion reaction. The net charges of each ion are obtained by standard Mulliken's manner,[24] and only the ions around the center of the cluster (Figure 6) are refereed for the calculation of net charges to avoid ambiguity associated with the presence of the cluster surface. The ionic positions for the cluster model are listed in Table 1. The lattice parameters for the calculation were cubic root of the cell volume of $La_{1/3}NbO_3$.[13] As mentioned above, because the changes of cell volume are negligible, [10] and the electronic structure changes with Li insertion are not due to the structural change, the calculations before and after Li insertion were carried out under the assumption of constant volume reaction, or both of the clusters have the same lattice parameters. In this cluster model, oxide ions are classified into three crystallographic positions, labeled as O1, O2, and O3. Figure 7 shows the arrangement of coordinated cations around three kinds of oxide ions, and each of the oxide ions is distinguished by coordinated A-site cations (for example, O1 has four neighboring La ions, while O3 is surrounded by four Li ions after insertion.)

Table 2 is a list of net charges before and after lithium insertion. The ionicity of each ion is about 50% of their formal values, except for the doped Li^+, and indicate strong covalent character. The net charges of Nb ions clearly decreased with lithium insertion, which indicates that the reduction reaction mainly occurs at Nb ions. This result is in good agreement with the XAS spectra in Figure 4b. On the other hand, net charges at O ions vary and are different at each position. The net charges of O3 surrounded by four Li ions are decreased after Li insertion, while O1 and O2 ions hardly changed their net charges. These discussions are also supported by the following discussion about the variation of electron distribution.

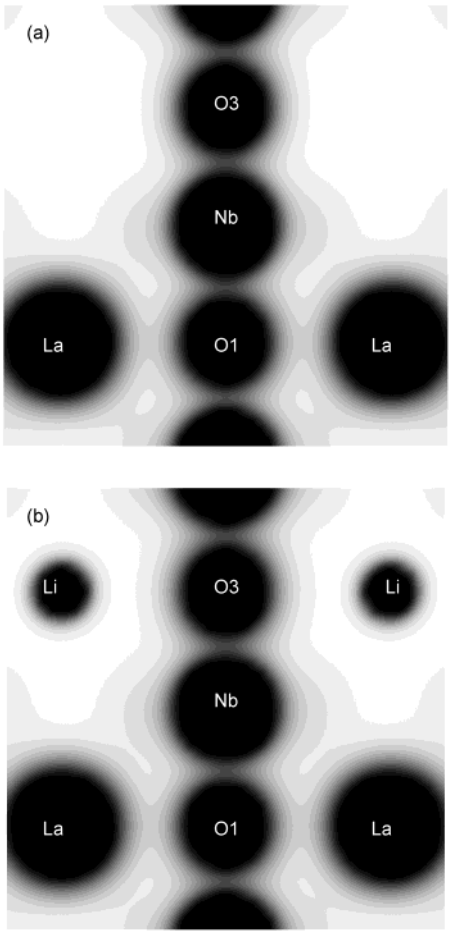

Figure 8. Calculated electron density of (110) plane for the samples (a) before and (b) after lithium insertion.

Table 2. Net Charges of Each Ion Obtained by First Principles Molecular Orbital Calculation Before and After Lithium Insertion

symbol/ atom	before lithium insertion	after lithium insertion	difference
La/La	+1.321	+1.456	+0.135
Li/Li		+0.791	+0.791
Nb/Nb	+2.67	+2.24	−0.43
O1/O	−1.122	−1.189	−0.067
O2/O	−1.309	−1.295	+0.014
O3/O	−0.89	−1.079	−0.189

Figure 8 shows the electron density distribution of (110) plane before and after the insertion. From the figure, quite strong covalent bonds exist between Nb and O ions, however the electron density is almost empty between Li and O atoms which indicates the existence of strong ionic bonds. Figure 9 exhibits the positive part of the difference in electron density before and after the

(23) Adachi, H.; Tsukada, M.; Satoko, C. *J. Phys. Soc. Jpn.* **1978**, *45*, 875.
(24) Mulliken, R. S. *J. Chem. Phys.* **1955**, *23* 1833.

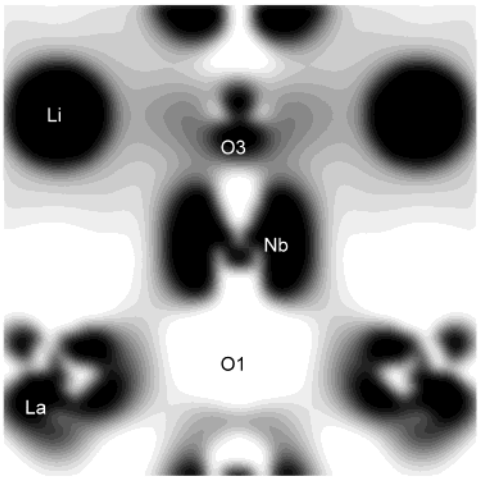

Figure 9. Positive part of difference in electron density before and after lithium insertion. Darker area indicates an increase in electron density.

insertion. The darker area in the figure corresponds to a greater increase in electron density after insertion of Li. The electron density around Nb and O3 (neighboring site of inserted Li) increases after insertion, while the electron density of O1 (without neighboring inserted Li) is not changed.

Accordingly, the change of electronic structure of oxide ions is not due to the reduction of Nb ions, but to the variation of ionicity of oxide ions introduced by Li ions with strong ionic character, since the electron transfer at oxide ions through the insertion of Li is strongly dependent on the existence of neighboring Li. The changes of net charges in O3 ion would correlate with those of O K-edge spectra with lithium insertion.

In conclusion, the XAS measurement and first principles molecular orbital calculation revealed that the oxidation states of La remained unchanged through the electrochemical lithium insertion, while those of Nb and O were changed with reaction. Furthermore, the charge compensation due to redox reaction mainly occurs at Nb cations, and the change of electronic structure of oxide ions is ascribed to the ionization due to the inserted lithium ions.

Acknowledgment. This work was supported by a Grant-in-Aid for Scientific Research on Priority Areas (B) (740) "Fundamental Studies for Fabrication of All Solid State Ionic Devices" from the Ministry of Education, Culture, Sports, Science and Technology. M.N. thanks the New Energy and Industrial Technology Development Organization for financial support of this work. The La L_{III}-edge XAS experiments were performed at the Photon Factory with approval of the High Energy Accelerator Research Organization (Proposal 2001G120), and Nb L_{III}-edge XAS and O K-edge XAS measurement were carried out at the UVSOR with approval of the Institute for Molecular Science (Proposals 13-843 and 13-876).

CM020741U